Research article

Effects of aging of radioactive fallout on timely decontamination of concrete using low and mild pressure washing

Katherine Hepler [a], Michael D. Kaminski [a,*], Noemy Escamilla [b], Matthew Magnuson [c]

[a] *Strategic Security Sciences Division, Argonne National Laboratory, 9700 S. Cass Ave., Lemont, IL, 60439, USA*
[b] *Department of Chemical and Biomolecular Engineering, University of Illinois, 1406 W. Green St., Urbana, IL, 61801, USA*
[c] *U.S. Environmental Protection Agency, Office of Research and Development, Center for Environmental Solutions and Emergency Response, 26 W. Martin Luther King Dr., Cincinnati, OH, 45268, USA*

ARTICLE INFO

ABSTRACT

Timely decontamination will reduce the consequences of a radiological contamination event. For this purpose, pressure washing can be rapidly deployed, but its effectiveness will change if the interactions between the surface and radionuclides changes as the contamination "ages" under the influence of time and precipitation. While effects of this aging have been reported for dissolved cesium, they have not been studied for radionuclides present as particulate, e.g., fallout. This work studied the effects of aging on decontamination with low (<280 kPa/40 psi) and mild (14,000 kPa/2000 psi) pressure washing, on concrete contaminated with surrogate fallout consisting of soluble Cs-137, 0.5 μm silica particles, and 2 μm silica particles. The samples were aged up to 59 days (time between contamination and decontamination) with and without simulated precipitation. The percent removal following decontamination of the soluble cesium decreased over the first ten days of aging until the removals were less than 10 % for both low and mild pressure washing. The particle decontamination was independent of aging time but decontaminating via mild pressure washing (>80 % particle removal) significantly outperformed decontaminating by low pressure washing by flowing solution across (parallel to) the contaminated surface (<25 % particle removal). The observed changes in decontamination efficacy are explained via measurements of the penetration depth of contaminants. For soluble cesium, the results compared favorably with prior studies and theoretical treatment of cesium penetration, and they yielded additional insight into the effect of washing pressures on decontamination. There are no comparable studies for particulate contamination, so this study resulted in several novel observations which are operationally important for timely decontamination of surfaces following a radiological incident. It also suggests an evidence-based pressure washing procedure for timely decontamination of soluble and insoluble radionuclides which can be used throughout the emergency phase and into the early recovery phase.

Environmental implication

Radioactive contaminated building materials represent a hazardous material requiring decontamination following an accident, act

---

of terrorism, or war which releases nuclear or radioactive material. The prevalence of concrete in the built environment emphasizes the importance of understanding the best methods of decontaminating such material to minimize environmental and societal damage. Since various forms of washing are frequently included in recovery planning, this paper presents for the first time a comparison between the use of low-pressure water and mild-pressure water wash down methods to decontaminate concrete samples of radioactive contamination. These results have direct implications on choosing strategies for environmental recovery.

1. Introduction

A radiological release such as a nuclear reactor accident can contaminate vast urban areas. International efforts established frameworks for remediating the built-environment following the Chernobyl and Fukushima nuclear reactor accidents [1–5]. Specific decontamination goals are not necessarily prescribed by these documents and will be site specific based on local concerns. However, a common theme is that timely decontamination will reduce the consequences of the incident in two main ways. First, such decontamination can restore access to roadways and buildings, such as hospitals, communications facilities, and water plants. Timely access to critical infrastructure will help reduce immediate consequences and shorten the timeline for the overall recovery to the incident. Second, freshly deposited radionuclides can be initially easier to remove, but, over time, the radionuclides interact with materials in the built environment under the influence of precipitation. This interaction, known as "aging" can make the radionuclides very resistant to decontamination, requiring aggressive, time-consuming, and expensive approaches. The aging effect occurs mechanistically by both the slow transport of the soluble radionuclides in a hydrated media [6] and the slow kinetics for sorption/desorption displayed by primarily micaceous minerals [7].

Decontamination techniques identified and refined before an incident will provide the most benefit. Though certain aspects of a release event will not be known until after the incident has occurred, there are certain commonalities among previous contamination events. For instance, because of its wide usage and abundance in spent fuel, cesium is likely to be a primary long-term contaminant. Depending on the release event characteristics, radionuclides may be found encapsulated in particles or in its soluble form [8,9]. Other more refractory elements, e.g., isotopes of plutonium, strontium, americium, iridium, are expected to precipitate as insoluble particulates (fallout) whose transport properties will be dictated by surface-surface interactions [8,10]. The physical form of the contamination will dictate the most suitable decontamination method since large fallout particulate contamination can be removed by methods such as washing with water [11,12] whereas soluble forms may be removed ineffectively by water [13]. Instead, soluble forms of the radioisotopes may require additives to enhance desorption of the radioisotopes from the surface [14–16]. While nuclear facility decontamination methods often prescribe harsh mineral acids or chelating reagents, use of such chemicals in the outdoor environment would be difficult due to chemical safety (mineral acids) or reagent cost (chelating agents). Studies on particulate forms focused on large millimeter sized fallout since they [11,12,17–20] sought to describe conditions for near ground zero fallout, which has been shown to consist of coarse-grained materials.

Many studies have described decontamination from roadway and building materials of soluble and particulate contaminations see Ref. [21] for review. Aside from investigations using physical methods of decontamination, most studies evaluated the use of water-based wash methods. Most of these past studies focus on the change in the initial activity (A_i) to the final activity (A_f) decontamination efficacy, most often expressed as: (a) the percentage removal via contamination, % $R = 100 * A_f/A_i$; or (b) the decontamination factor, $DF = 1/(1-A_f/A_i)$. Few studies have examined how aging affects decontamination [6,22–25] for soluble radionuclides. No study to date has monitored the decontamination efficacy on the aging of soluble and fine particulates that characterize far-field fallout. To support timely decontamination, specific studies of the effect of aging for soluble and particulate contaminants for specific decontamination techniques are needed.

There are few readily deployable techniques for wide area decontamination of roadway and building materials in the days or weeks following a release event aside from water wash methods. Two options are low-pressure (<280kPa/40psi, at the low end of household water pressure and similar to wash pressures by firehose, garden hose, or the action of heavy rain) and mild pressure washing (such as a 14,000 kPa/2000 psi gas or electric pressure washers found at local home supply stores). Pressure washing systems tend to use much less water than low pressure systems and generate much less liquid waste. Note that "high" pressure washers with 10–100 times the "mild" pressure are available commercially but not as common or accessible as the mild pressures here. The higher pressures tend to ablate the surface so have a different decontamination mechanism than lower pressures which remove the radionuclide from the surface without destroying the surface.

Overall, the goal of the study is to investigate the effects of aging and optimize the potential of deploying water wash methods for wide area decontamination specifically employing pressurized washers in a manner that is non-destructive, conserves water resources, and minimizes solid waste generated. Pressure washing for radionuclide decontamination is not new [21], and practical considerations for their application have been discussed [26,27]. However, this work is novel in that it investigates important variables such as the impact of Cs-137 solubility as a function of the time after release, including any rainfall that may have occurred prior to decontamination. Since Cs-137 or other radionuclides may be bound inertly to particles, another novel variable was the size of such particles. Other variables relating to radionuclide migration and decontamination as a function of washing conditions are also investigated.

2. Materials and methods

2.1. Concrete samples

All tests used concrete monoliths made with a ratio of 250 g Quikrete concrete mix (No. 1101 Standard 4000 psi, Atlanta, GA) to 21

mL of deionized water (18.2 MΩ-cm). Molds 2.5-cm tall with 3.8-cm diameters were filled with this mixture and then the concrete cured for 14 days with the samples sprayed with deionized water periodically and sealed in plastic container to maintain humidity. The samples were removed from the molds, cured for another 13 days, allowed to equilibrate with ambient lab humidity (65–75 % R.H.), and then the perimeter and bottom of the samples were epoxied (Devcon Quickdry Epoxy, Danvers, MA).

2.2. Surface roughness

The surface roughness of two coupons were measured using a Keyence VR-3000 microscope for a sample with visually 'average' surface roughness and for a sample with noticeable surface irregularities. These measurements suggest most samples had a surface roughness range between 0.3 mm and 0.5 mm. Sample roughness consisted of cupping of the sample surface (depressed center, raised edges) and each sample's unique roughness features marked by an inconsistent smooth coating of the cement phase.

2.3. Contaminants and contamination of samples

Samples were contaminated with soluble Cs-137 (in-house stock dissolved in dilute nitric acid) and two sizes of radiolabeled surrogate fallout particles. The surrogate fallout particles, spherical silica particles sized 0.5 μm and 2 μm, were radiolabeled according to the procedure described in Ref. [28]. The particles were radiolabeled with ^{152}Eu (approximately 1 mCi/mL in 0.5 M HCl, Eckert and Ziegler, Valencia, CA) and ^{153}Gd (1 mCi/mL in 1 M HCl, Eckert and Ziegler, Valencia, CA). Leaching tests described by Jolin et al. [28] were completed by mixing the radiolabeled particles in 0.5 M HNO$_3$ or dilute SSDX-12 soap solution for 1-h, and the tests showed very good adherence of the radiolabel to the particles (for 2 μm particles: 6.2 % loss in HNO$_3$ and 0.7 % loss in SSDX; for 0.5 μm particles: 4.3 % loss in HNO$_3$ and 3.1 % loss in SSDX).

Samples first received 200 μL of soluble Cs-137 spike solution (~2000 CPM in deionized water), then 100 μL of 0.5 μm particle solution (~200 CPM ^{153}Gd-labeled particles in ethanol), and finally 100 μL of 2 μm particle solution (~200 CPM ^{152}Eu-labeled particles in ethanol). Between the applications of each solution, the samples dried for at least 30 min. Sample activity was measured using an Ortec GEM-35190-P HPGe detector (calibration checked against a standard ^{60}Co check source, 33.9 % relative efficiency at 1.33 MeV) monitoring the 662 keV photopeak for ^{137}Cs, the 121 keV photopeak for ^{152}Eu, and a region of interest (ROI) combining the 97.6 keV and 100 keV photopeaks for ^{153}Gd. All samples were counted in the same geometry and orientation. The percentage of activity removed (decontaminated) was calculated from the total counts in the photopeak before and after decontamination. The uncertainties for each data point were calculated as the standard deviation between the five samples for each test condition. The counting error was propagated through the average calculation, but the resulting errors were less than the standard deviations.

2.4. Aging conditions

After contamination, samples were "aged." That is, they were kept in ambient laboratory conditions between 1 and 59 days before decontamination or depth profile measurements (average 20 °C and 65–75 % R.H.). While aging, half of the samples received simulated precipitation via "modified stormwater" (described in the next paragraph), as rainfall or snowmelt would be expected to become stormwater after contacting a concrete surface. To apply the "precipitation", every 2–4 days, 1 mL of modified stormwater was pipetted onto sample surfaces in intervals of 100–200 μL over 3–5 h. The timing and volume of "applied precipitation" was based on Chicago, IL rainfall weather records [29]. Solution was not allowed to spill over the sides of the sample.

The composition of modified stormwater followed [30,31], except without the zinc and copper components. Briefly, the applied precipitation contained the following salts added to 45 mL of deionized water: 9.1 mg of magnesium sulfate anhydrous (Sigma Aldrich, St. Louis, MO, USA), 90.9 mg of potassium nitrate (Fisher Scientific, Pittsburgh, PA, USA), 91.3 mg of sodium nitrate (Fisher Scientific), 126.5 mg of potassium chloride (Fisher Scientific), 299.3 mg of sodium chloride (Fisher Scientific), and 46.9 mg of calcium chloride dihydrate. The concentrated salt solution sat overnight before being diluted to 1 L with deionized water. Ten milliliters of modified stormwater solution were analyzed by inductively coupled plasma mass spectrometry (PerkinElmer NexION 2000 Inductively Coupled Plasma Mass Spectrometer, relative uncertainty ± 10 %, Akron, OH, USA). Samples were prepared by dilution with nitric acid (Optima grade) to achieve 1 % acid, and concentrations reported in Table 1 are corrected for dilution.

2.5. Decontamination of concrete samples

Samples were decontaminated either by passing a stream of water over the sample face (low-pressure flow test) or passing the face under pressurized water flow (mild-pressure wash test). Both tests used a 0.1 M KCl wash solution (111.82 g Nature's Own Potassium Pool Cubes, >99 % pure, Home Depot, IL in 14.95 L of tap water) to enhance ion exchange reactions with the cesium sorbed onto the

Table 1
Mass concentrations and molarity results from ICP-MS analysis of applied precipitation, with relative uncertainty of ±10 %. The sulfate mass concentration was calculated from the magnesium mass concentration.

	Mg^{2+}	K$^+$	Na$^+$	Ca^{2+}	SO$_4^{2-}$
Mass concentration (μg/L)	2.1 x 10^3	1.1 x 10^5	1.6 x 10^5	1.3 x 10^4	8.2 x 10^3
Molarity (mmol/L)	0.085	2.8	7.1	0.32	0.085

surface [32] and to neutralize surface charges that might prevent the detachment of fallout surrogates [33]. During low-pressure flow tests, samples were decontaminated by pumping (Fischer Scientific Mini-Pump Variable Flow) 0.1 M KCl solution at 100 mL/min onto the top of a sample-holder conduit tilted about 30° downward for 15 min similar tests were performed in Ref. [34].

The pressure wash system is described elsewhere [35]. The system was outfit with a 13,790 kPa (2000 psi) Ryobi electric pressure washer (4.52 L/min, Anderson, SC) and a 15° nozzle (size 2, McMaster-Carr, Elmhurst, IL). The nozzle was held 27 cm from contaminated surfaces during power washing. This study used a linear cleaning rate of 5 mm/s, which resulted in 0.1 M KCl solution contacting contaminated samples for about 5 s. Samples were decontaminated in groups of two or three. Importantly, the impact pressure was significantly lower by about a factor of 10 than reported in (Jolin et al., 2019) where that study held the wand 15 cm from the sample surface.

2.6. Depth profile measurements

In addition to characterizing the relationship between decontamination efficacy and contaminant aging through decontamination tests, the subsurface migration of contaminants was measured for two concrete monolithic samples from each aging group that were not decontaminated. The procedure for determining depth profiles in this work was modified from previous studies [6]. Before each depth profile test, the sample dimensions were measured using a caliper with precision 0.01 cm and weighed (Mettler AT261 scale with 0.01 mg precision). The surface of concrete samples was ground against strips (5.5 cm by 11 cm) of 100-grit sandpaper (3 M, Grainger, IL) to remove surface material, and then weighed again. This strip of sandpaper with the contaminated surface material was rolled, placed in a plastic gamma counting tube, and counted for 30 min for the 662 keV photopeak for ^{137}Cs, 121 keV photopeak for ^{152}Eu, and region of interest (ROI) combining the 97.6 keV and 100 keV photopeaks for ^{153}Gd (PerkinElmer Minaxi γ Auto-Gamma Counter Model A5550 NaI well-type detector, Wiz2, 47 % efficiency for ^{137}Cs, Shelton, CT). Each concrete monolithic sample had at least 15 layers of surface material removed. In addition, the concrete sample was counted on the HPGe detector before and after top-surface removal to determine the fraction of activity removed. The steps to correlate measured layer counts to total activity removed measured by the HPGe detector has been described elsewhere [35]. Uncertainties in layer thickness and activity removed were calculated (see Supplemental A for details) by propagating system uncertainties (e.g., scale uncertainty, counting error, and dimension measurement uncertainty).
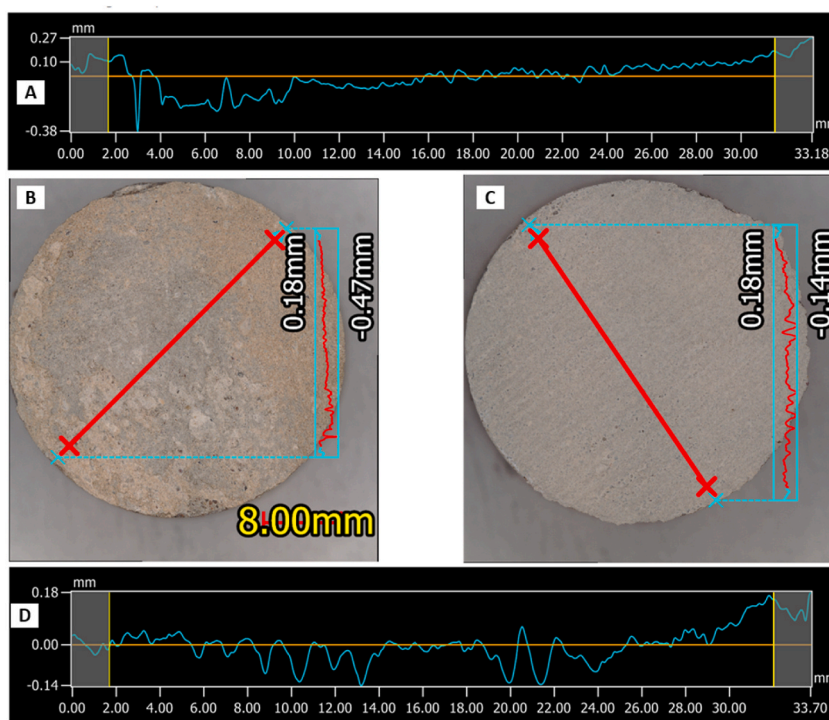
Fig. 1. A: Line (red) roughness profile of the sample in "B" from lower left to upper right quantifying the depth of some ridges. B: The light-grey spots in the bottom half of the coupon face are pitting of the coupon surface. C: The faint beige-tinted lines running from the bottom left to the upper right of the coupon face are ridges in the coupon surface. D: Line (red) roughness profile of the sample in "C" from lower right to upper left quantifying the depth of some ridges. (For interpretation of the references to colour in this figure legend, the reader is referred to the Web version of this article.)
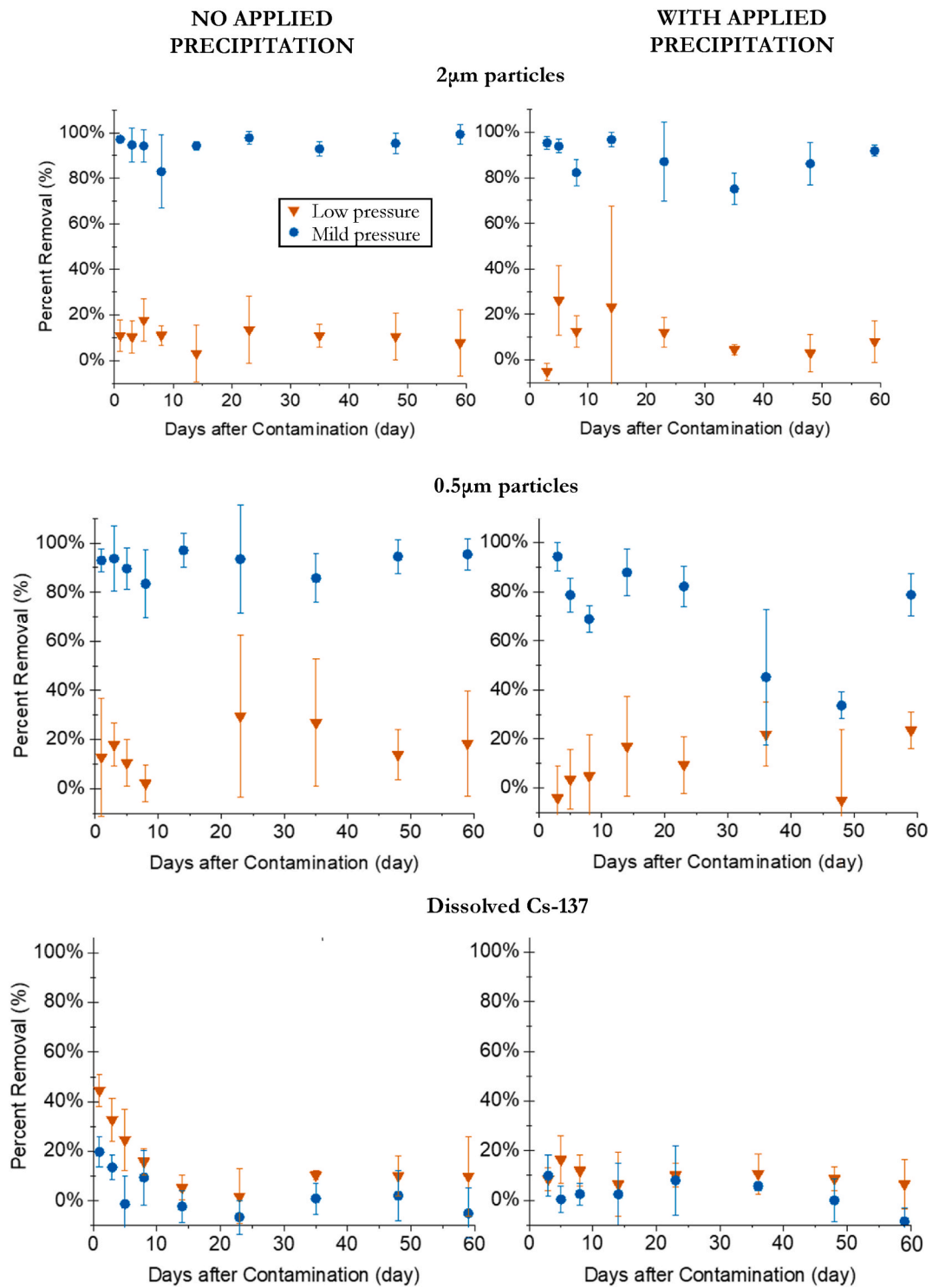
Fig. 2. Mild pressure wash (circles) and low-pressure flow (triangle) decontamination results using 0.1 M KCl solution for aging with no precipitation (left column) and aging with precipitation (right column) for 2 μm (top), 0.5 μm (middle) particles and dissolved Cs-137 (bottom) contaminants. (The error bars on each data point show the standard deviation for the five samples for each test condition. The counting error was propagated through the average calculation, but the resulting errors were less than the standard deviations. The large error bars for some data points were a result of relatively low total counts in the original photopeak.)

3. Results and discussion

3.1. Surface roughness

The surface roughness of two visibly different samples provided some insight into interpreting the results of subsequent decontamination and contamination depth experiments and the effect of aging. The surface of the first coupon (Fig. 1B) was visually "rougher" than the second coupon (Fig. 1C), which appeared smooth across the surface. The "roughness" of the coupon in 1B covered ~50 % of the surface and was characterized by numerous porous openings in the cement phase. Approximately 10 %–20 % of coupons tested had areas of roughness like the lower portion of the coupon (Fig. 1B). The line roughness analysis (Fig. 1A) showed a range of 650 μm from the highest to lowest point along the line at the bottom left where there was a visible rough patch. The numerous peaks and valleys in the plot denote pores that range in extreme from 525 μm deep (deep thin pore at 3 mm along the line plot, Figs. 1A), 2 and 800 μm wide (at 4–7 mm along the line plot) to more common pores of 25–60 μm deep and 160–400 μm wide on the smoother half of the coupon to the upper right of the scan line in Fig. 1B.

The second coupon was visibly smoother in appearance (Fig. 1C). The surface had a smoother appearance with small, parallel ridges along its surface. Some of these ridges are apparent in the line roughness graph (Fig. 1D). Between 20 % and 30 % of coupons were estimated to have similar ridges along part or all their surfaces. The numerous peaks and valleys in Fig. 1D correspond to pores from 10 to 160 μm deep to 170–670 μm wide, in contrast to the rough coupons.

The line roughness graphs for each sample in Fig. 1 and in all samples in this study show slightly concave surfaces (cupping), where the roughness plots show the raised profiles at the extreme ends of the scan line, in addition to each sample's unique roughness features. For the coupon in Fig. 1C, there is very little cupping (estimated ~20 μm) at the lower right edge of the coupon. However, there is cupping of about 180 μm along the upper left edge of the coupon. From these images and visual observations of the other coupons used in testing, the extent of cupping varies both between coupons and can also be asymmetric on a single coupon.

In total, information from this technique leads to the following conclusions. All coupons display gross open pores that penetrate 10's to 100's of micrometers into the surface and 100's of micrometers wide, both orders of magnitude larger than the diameters of the surrogate fallout particles under investigation here. Thus, to decontaminate the coupon, sufficient external force would be required to overcome surface adhesion forces and enough water provided to sweep the particles from the test surface. Both the low-pressure flow test and pressurized spray test provide orders of magnitude more water than is necessary to fill the cupping volume and provide means for sweeping the particles form the surface. The cupping volume is at most 0.2 mL/cm^2 of coupon while the low-pressure flow test passes 1200 mL/cm^2 and the pressurized spray passes 11 mL/cm^2. However, the next section shows that despite sufficient water volume, the low-pressure flow conditions are not sufficient to overcome adhesion forces and sweep the particles from the surface.

3.2. Decontamination

Decontamination tests compared the efficacy of the mild pressure wash with a low-pressure wash to mimic the conditions of a pressurized washer and fire hosing/the action of water runoff, respectively as wide area wash techniques. Decontamination results for samples aged between 24 h and 59 days (Fig. 2) show that the particles exhibited modest removal ($\leq$30 %) during low pressure flow tests but had much higher removals, sometimes quantitative within experimental error at the 95 % confidence level, using mild pressure wash.

Across all days and regardless of precipitation, the 2 μm particle removals after mild pressure washing compared to low-pressure flow decontamination were significantly different (p = 1 x 10^{-17} without precipitation and p = 2 x 10^{-10} with precipitation) from a two sample *t*-test with uneven variances at 95 % confidence level (Microsoft Excel), and the removals were within experimental error over time (Fig. 2 top). The 2 μm particle removals averaged greater than 75 % for every mild pressure wash test. In comparison, the removals averaged less than 25 % for all low-pressure flow tests. The difference in particle removal between the low-pressure flow tests and mild pressure wash tests indicate a physical removal mechanism for the particles. Because the applied pressure in this work is around ten times less than that in Ref. [35], it is likely minimal surface material was removed. In fact, microscopic examination of the sample surface after mild pressure washing revealed that the cement top-surface was still intact with no aggregate visible. Jolin et al. [35] showed that the cement surface layer was absent and exposed aggregate characterized the concrete surface after his high-pressure wash tests. The high particle removal efficacy with minimal surface ablation supports the idea that particles have settled into depressions across the sample surface but are readily accessible by solution sprayed normal to the surface. Comparing the removals of 2 μm particles from the samples aged with and without applied precipitation (i.e., simulated rainfall in the form of modified stormwater), no trend is observed, and the results out to 59 days is not statistically different between samples aged with and without precipitation.

The 0.5 μm particle removals exhibit many of the same trends and statistical differences (p = 8 x 10^{-9} without precipitation and p = 8 x 10^{-5} with) as the 2 μm particle removals over time and between decontamination method (Fig. 2, middle). Two points have very large errors on account of low initial photopeak counts. Low-pressure flow tests removed 0.5 μm particles with less than 30 % efficacy for all aging conditions. Mild pressure washing removed on average more than 80 % of the 0.5 μm particles on time-only aged coupons. In comparison, the average removals after mild pressure washing precipitation-aged coupons varied between 35 % and 94 %. The 0.5 μm particle removals applying pressurized wash solution to coupons, aged with either 12 or 16 precipitation applications (over 36 or 48 days, respectively), yielded average removals 30 %–50 %. The 0.5 μm particle removals indicates the 12 precipitation application coupons behaved differently from one another. However, the small deviation in the 16 precipitation applications removals shows the opposite, suggesting this difference may have arisen from low initial photopeak counts, rather than from a phenomenon related to

aging.

The differences between the 0.5 and 2 μm is likely related to the physics of surface-particle forces and the roughness features of the concrete surface. It is recognized that particles ~2 μm represent a transition between those that are easily removed and those that are difficult to remove using non-contact methods including pressurized water [36]. This difficulty is explained by the presence of a fluid boundary layer that prevents the transfer of energy from the fluid velocity to particle surface to overcome adhesion forces. These adhesion forces are described by van der Waals interactions, electrostatic forces due to surface charges, capillary forces, and drag forces [33]. Briefly, dynamic van der Waals adhesion forces are greatly reduced in the presence of water but are directly proportional to the particle radius, e.g., the magnitude of these weak electrostatic force is four times higher for a 2 μm particle than for the 0.5 μm particle. The electrostatic force due to permanent surface charge effects is greatly reduced in the presence of the ions in solution. For instance, polystyrene has a highly negative surface charge in deionized water, but this charge is severely depressed in 0.1 M KCl to the point that van der Waals forces become the dominant electrostatic force [37]. Capillary forces would be important in high humidity where a layer of water molecules surround the particle and anchor it to the surface onto which the particle sits. However, once the area becomes flooded with water, this force becomes unimportant. In total, the presence of salt in the water would reduce the electrostatic and capillary forces to negligible levels and leave the van der Waals forces as the dominating adhesion force.

To overcome the van der Waals force, the drag force due to passing water must be larger. The drag force is proportional to the square of the local velocity and the projected frontal area of the particle to the incoming fluid normalized by the thickness of the fluid boundary layer δ [36] between the laminar sublayer and turbulent flow fields. Thus, the drag force would be much larger for larger diameter particles that extend further into the turbulent flow field than smaller particles, which may reside entirely in the much slower moving laminar flow sublayer. For example, a 1000 psi water spray (free flow velocity = 100 m/s) produces a laminar flow regime <10 m/s that extends about 1 μm from the surface. For 0.5 μm particles the result is a drag force 10–100 times smaller than for 2 μm particles [38]. From extremely flat optical surfaces, high pressure jet spraying (4000 psi) is recommended for particles 0.5 μm and smaller [36]. Microscopic surface roughness tends to dramatically reduce the van der Waals adhesion force and so should facilitate the removal of small particles under these conditions unless the particles rest between the asperites of the rough surface [39].

Another complicating mechanism that may explain the reduction in 0.5 μm particle removal is due to the presence of micropores much smaller than the gross surface inhomogeneity displayed in Fig. 1. It is plausible that the 0.5 μm particles migrated into micropores deeper than the 2 μm particles and experienced stronger adhesion forces through multiple contact points within the pores and became "hidden" from the fluid flow [39]. The combination of the applied precipitation and moderate relative humidity (65–75 % R. H.) while aging the contamination on the 16 precipitation applications coupons may have facilitated the migration of particles far enough into these micropores to not be removed during testing.

In summary, the low-pressure flow conditions provided insufficient drag force from the impinging spray to overcome van der Waals forces for both particle sizes examined here. However, the high-pressure spray was able to overcome these forces except in some of the more aged coupons containing the 0.5 μm particles, presumably through transport of these smaller particles into micropores in the samples.

The removal of dissolved Cs-137 (Fig. 2, bottom row) was different than experimental error for samples that experienced no precipitation when the contamination was aged less than eight days. The flow tests showed greater removals of cesium than pressurized washing during this time frame, but similar removals across the entire time frame. This suggests an effect of kinetics. Kaminski et al. [34] reported earlier the kinetics of decontamination and showed how decontamination gradually increased as the coupon was exposed to Cl$^-$ solutions out to 60 min. However, Fig. 2 shows that after 5–10 days, the cesium removals are low (≤12 %) regardless of decontamination pressure.

Cesium exhibited different trends than the particles because it is a soluble contaminant. The cesium removals following pressurized washing with 0.1 M KCl averaged less than 20 % for all aging experiments, including those with precipitation. This observation could be related to one, or several, of the following. First, cesium migrates under the influence of water into the concrete matrix which is frequently reported. This migration starts to occur when precipitation is applied, hence removals are lower for initial time points. Second, the pressurized washing experiments removed a fine layer of surface material, onto which approximately 0 %–15 % of the cesium was adsorbed. The amount of cesium adsorbed onto the removable surface material did not change over time. Third, the amount of cesium close enough to the sample surface to chemically interact with the pressurized wash solution did not change throughout the 59 days. These later two possibilities are very similar, except the first is describing physical removal of fine surface material and the second describes a rapid chemical interaction between the wash solution and cesium fixed on or near the sample surface. The slight increase in cesium removal for the 1-day aged, no precipitation tests compared to all other data points, weakly supports the second hypothesis.

Unlike the pressurized washing tests, the low-pressure flow tests primarily rely on a chemical removal mechanism. The largest cesium removals were observed for the 1-day aged, no precipitation samples after decontamination using by low-pressure flow tests. The cesium removal significantly drops, within experimental error, between samples that have been aged one day and those that were aged eight days. As the samples are allowed to age, cesium migrates into the subsurface. However, the depth accessed by the wash solution during the low-pressure low tests does not change and may be several millimeters in depth (see Supplemental B). Yet, the removal data in Fig. 2 shows non-zero average removals after sixty days. Thus, some of the cesium on the samples must stay at a depth that can be accessed by the wash solution during low-pressure flow tests. This suggests that, as a potential decontamination technique following a wide-spread dispersal event, low-pressure flow application of wash solution should be applied within the first ten days after an incident to have decontamination efficacy above 10 % for soluble cesium contaminated concrete.

3.3. Depth-profile measurements

The contaminant depth profiles (Figs. 3–5) indicate most particles have insignificant subsurface penetration regardless of number of precipitation applications (Fig. 4) or aging (Fig. 5). This insinuates that precipitation application did not promote particle penetration into the coupon. However, data in Fig. 2 suggests the applied precipitation moved some particles into the micropores inaccessible to water flow. Instead, particle depth profiles were dependent on the sample surface roughness and uniformity of contamination as we explain below. Most of the cesium can be found in the first 1 mm of the subsurface after 60 days of aging with precipitation events in moderately humid environments (65–75 % R.H.). Cesium depth profiles were also dependent on surface roughness and uniformity of contamination, but to a lesser degree. Unlike the particles, there was a difference between samples aged with precipitation events and those aged only over time. These conclusions were drawn by comparing the 34 depth profiles to each other rather than relying on comparisons within one figure or aging time. First, the effects of sample surface roughness on depth profiles are discussed, then the effects of the number of precipitation applications on contaminant penetration, and finally a comparison of the results to previous literature and simple theoretical treatment of cesium diffusion in concrete. Select profiles are paired together in Figs. 3–5 that demonstrate the features discussed.

There is a discrepancy between the plotted depth and the actual depth. While removing the first few layers, the sandpaper only contacts the peaks of the coupon surface. The peak height was mainly associated with cupping along the outer few millimeters of the coupon face. As the edges were scraped away, the sandpaper started to contact the central areas of the coupon face. The degree of sandpaper contact with the different parts of the coupon face was qualitatively noted by observing the percentage of aggregate exposure throughout the test. The aggregate was gradually exposed working from the edge of the coupon inward (see Supplemental C, Fig. S1). Once aggregate was visible on most of the surface, the calculated depth of subsequent layers was more accurate. This behavior, caused by the degree of coupon surface dipping, would not be present for large concrete surfaces. Cracks and other major surface irregularities aside, the estimated penetration depth of contaminants on large concrete surfaces would be less than predicted by these experiments. Thus, the decontamination efficiencies for realistic surfaces may be larger and these studies provide a more conservative decontamination efficacy, as discussed in more detail below.

Examining the particle depth profiles in Figs. 3–5, almost all particle activity is found within the first 200 μm–400 μm, within the range of gross pore size depth observed in Fig. 1. Removal by sandpaper is expected to be unrelated to particle size; both particle sizes were observed to be removed similarly, so only the 2 μm is shown. Precipitation had no discernible effect. There were two primary shapes for particle depth profiles: exponential decay and linear. The adhesion of the particles to the coupon surface, coupon surface roughness, and uniformity of contamination likely dictated which trend the penetration profile followed. The depth profiles showed no dependence on aging time or method. Because all coupons exhibit some degree of surface cupping, particles in the center of the coupon would not be removed within the first few layers. If the cupping was the primary source of roughness for a sample and the particle contamination was uniform in the radial direction, then particle penetration profiles would be more linear (Fig. 3, left plot, blue and yellow lines, Fig. 5, left plot, blue and orange lines). Coupons that yielded particle depth profiles following more of an exponential decay had particle contamination that was removed within the first few layers (Fig. 3, left, orange and grey lines, Fig. 5, left, yellow and grey lines). This pattern likely indicates a smoother and flatter coupon surface and that a greater percentage of the coupon surface was contacted by the sandpaper during removal of the initial layers.

Like the particles, the dissolved cesium penetration profiles were affected by the surface roughness of the sample (Fig. 3). Increased coupon cupping resulted in more linear cesium penetration profiles (Fig. 3 yellow and blue lines). Conversely, smoother samples with shorter aging times had cesium contamination profiles shaped like an exponential decay (Fig. 3 orange and grey lines). Some coupons had less cesium removed in initial layers, resulting in a flattened depth profile near the surface. This is a product of coupon cupping and the contamination procedure. When contaminating the coupons, solution was deposited a few millimeters from the coupon edge and
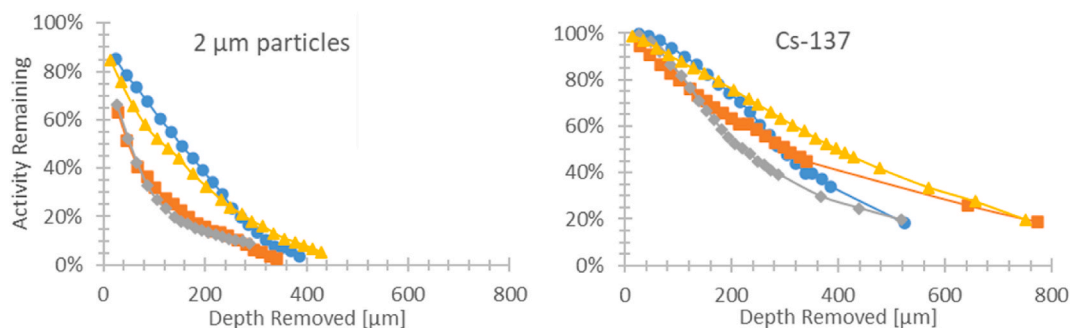

Fig. 3. Effect of surface roughness effects on activity remaining as a function of depth removed. The orange and grey data are from relatively flat surfaces, and the curves are more exponentially shaped, reflecting that the grinding method removes surface layers more easily, compared to the blue and yellow data which are from relatively rough and cupped coupon surface. The more rough/cupped surface requires deeper layer removal to remove the particles (left) and dissolved Cs-137 (right). The effect appears independent of applied precipitation, as blue and grey received no precipitation applications, whereas yellow and orange received 12 or 16 applications, respectively. (For interpretation of the references to colour in this figure legend, the reader is referred to the Web version of this article.)
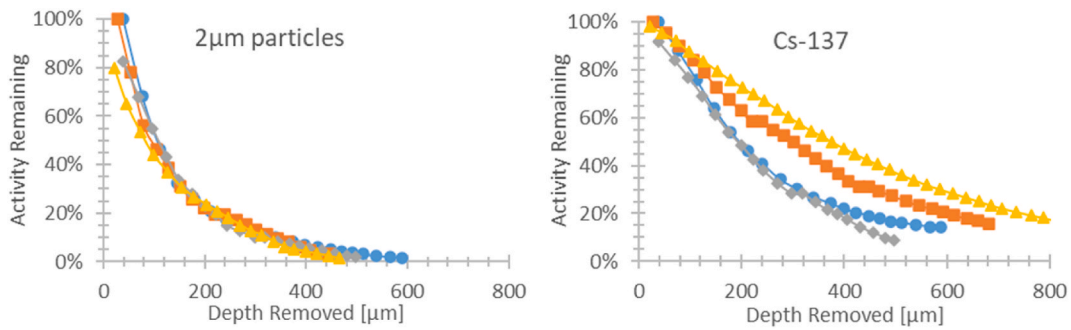
Fig. 4. Effect of precipitation versus no precipitation on activity remaining versus depth of surface removed. (Left) Duplicate coupons of samples with 2 μm particles (left) and soluble Cs-137 (right) with precipitation (orange and yellow data, eight precipitation applications) and without applied precipitation (blue and grey). (For interpretation of the references to colour in this figure legend, the reader is referred to the Web version of this article.)
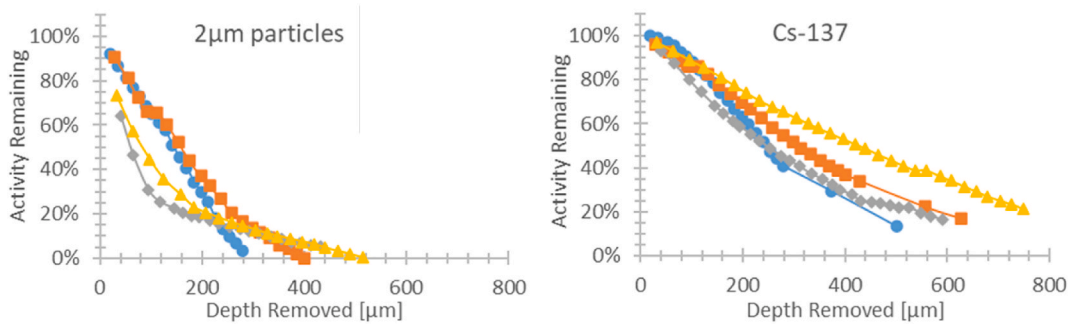
Fig. 5. Effect of number of precipitation applications on activity remaining versus depth of surface removed. The orange and yellow correspond to 3 and 20 precipitation applications, respectively. The blue and grey data were collected from samples without precipitation application but held for the same amount of time as the orange and yellow, respectively. (For interpretation of the references to colour in this figure legend, the reader is referred to the Web version of this article.)

inward. The solution spread close to the edge of the coupon but not always completely to the edge. If coupons had little cesium deposited near the edge of the coupon, the initial layers would contain minimal cesium for cupped samples. The flattened beginning of cesium contaminant profiles may be less pronounced for coupons that experienced rainfall events in the form of applied precipitation because rainwater promotes cesium diffusion. In all, due to surface roughness, the depths needed to remove contaminations suggested by the figures are a conservative estimate, and the contamination is likely retained at depths much shallower than indicated by Fig. 4

Table 2
Cesium depth profile data in concrete at different test conditions [6,35,40]. $F_{Removed}$ is the percent of activity removed following an experiment. Based on the figures in Ref. [6] and comparison to similar experiments, the two values exceeding 2 mm were likely due to excessive coupon surface roughness.

		[6]		[40]	[35]
		$F_{Removed}$ = 90 %		$F_{Removed}$ at 70 μm	$F_{Removed}$ = 80 %
Relative Humidity		30 %	87 %	Unknown	20 % ± 5 %
Days Aged	Sample				
1 day	a	2590 μm	300 μm	21 %	150 μm
	b	240 μm	600 μm		
7 days	a	240 μm	760 μm		
	b	5200 μm	600 μm		
8 days					100 μm
9 days				55 %	
14 days	a	240 μm	600 μm		
	b	280 μm	370 μm		
28 days	a	500 μm	443 μm		
	b	380 μm	730 μm		
90 days				57 %	

for which the coupons used were visually of typical variability in the study.

3.4. Comparison of cesium penetration to previous literature and to theoretical treatment

Supplemental section B presents a theoretical approximation of cesium penetration that agrees with the results presented above. In summary, the limited solution penetration in samples can be explained by concrete's low water sorptivity, diffusivity, and permeability. The theoretical approximation might overestimate the actual cesium penetration depth because actual concrete contains aggregate and unsaturated media, which are difficult to treat theoretically. Indeed, the penetration depth is theoretically estimated to be 2.4 mm, whereas the observed in this study was ~1 mm at most. Reassuringly, this penetration depth of cesium found in this work is also comparable and within the range of values found by five other studies using the same method to generate depth profiles. Table 2 summarizes the findings of cesium penetration for studies on non-saturated concrete and lists different test conditions. The data from Maslova et al. [6] clearly show the relationship between relative humidity and cesium penetration. As the relative humidity during aging increases, the rate of cesium migration into the subsurface increases. Thus, the studies by Jolin et al. [35,40] were performed at low relative humidity and showed minimal subsurface penetration of cesium. As a "worst-case" scenario comparison, penetration of cesium was recorded in water-saturated cement at 25 °C. After exposing one side of a coupon to cesium solution for thirty days, the cesium was mostly found within 1 mm of the surface [41,42]. The relative average humidity in the present study averaged 65 %–75 %. Most of the cesium profiles measured after less than 34 days of aging found 80 % of the activity within the first 600 μm. Even after 59 days of aging with or without precipitation events, the cesium only migrated approximately 700 μm–900 μm into the subsurface.

Two studies using coarser depth increments and longer aging times also indicate cesium migrates slowly through concrete. A U.S. EPA study examined the effects of rainfall on contaminant removal and penetration after weeks of aging [30] with half the samples experiencing a "rainfall" event. Samples were aged in low humidity environments prior to rainfall (about 20 days) and high humidity (≥90 % R.H.) for about 20 days after half the samples received rainfall. Depth profiles were analyzed using laser ablation ICP-MS to remove surface material in 100 μm increments. Most of the cesium contamination was found within 300 μm of the surface for control samples and within 500 μm for samples experiencing rainfall (based on estimates from activity distribution charts) [30]. Another study examined cesium penetration in concrete after more than two decades of aging. The samples, taken from Pripyat, Ukraine were analyzed by slicing them into 5-mm thick disks and measuring the activity of each disk. Greater than 90 % of the activity was found in the upper 5 mm of most concrete samples [43].

4. Conclusions and practical implications

This study provides additional information on how the decontamination efficacy of two washdown methods changes with respect to the contaminant form (soluble vs. particulate), contaminant-aging time, and contaminant aging conditions on concrete surfaces. For soluble cesium, the results compared favorably with prior studies and theoretical treatment of cesium penetration, and the results yield additional insight into the effect of washing pressures on decontamination. There are no comparable studies for particulate contamination, so this study resulted in several novel observations which are operationally important for timely decontamination of surfaces following a radiological incident.

First, with short aging times, soluble cesium was better removed by low pressure flow tests because of the extended contact time with the ionic wash solution, but efficacy rapidly decreased with aging. That is, applying low pressure flow across the cesium contaminated surface became ineffective (≤~ 10 %) after ten days of time-only aging or two precipitation events. The rapid drop in cesium decontamination efficacy suggests that operations by available equipment and operators using best practices in sources like [26] *immediately* after fallout has settled may be critically important in reducing long term decontamination needs. The ineffectiveness of the decontamination methods to remove cesium after extended aging times was attributed to subsurface migration, which is supported by the depth-profile results.

Second, by contrast, particle decontamination was mostly independent of aging time and aging method. For the surfaces investigated, it is likely that the aging conditions did impact the interaction between the surface and the particles. This occurred despite marked differences in the surface roughness, even when the depths of the ridges and depressions far exceed the particle sizes. These results strictly may only apply to these concrete samples, but since the sources of the physical forces may be common to other concrete, this result provides some assurance that decontamination of particulates may not need to proceed on as strict of timeline as for soluble cesium. When cracks and fissures are present in the concrete, pressure washing may be ineffective since the pressure and/or flow may not reach deep within such cracks.

Third, contaminants in particle form were better removed via mild pressure washing rather than low pressure techniques. Likely, even the mild pressure has sufficient fluid force to overcome adhesion forces and access particles that have settled into surface depressions of the concrete. Low pressure wash techniques are expected to be effective on smooth, impermeable hard surfaces like glass, plastics, metals, and painted surfaces especially when combined with wiping techniques [44–48]. In these cases, the wiping can supply considerable mechanical pressure. This suggests that low pressure decontamination wash techniques such as fire hosing, natural rain events, or surface runoff will result in poor decontamination factors for particle fallout decontamination on concrete –a rough, permeable surface. Thus, if such low pressure techniques are used, site specific specification of decontamination may be required.

Taken together, these observations logically suggest a technically sound protocol for performing wide-area decontamination that minimizes surface damage from excessive pressure washing, conserves water resources, and minimizes solid waste generated. In such a protocol, particulate fallout is first mobilized by a short application of mild pressure washing. Next, a longer application of low-pressure wash mobilizes the dissolved cesium. The longer application of low-pressure wash will also ensure that there is sufficient

water to carry the particulate contamination mobilized by the mild pressure wash to the area that wash water is collected. (Disposal of this collected water is a separate, detailed topic discussed elsewhere, e.g., see Ref. [27].) Then, if needed, higher wash pressures could be used to ablate the surface to decontaminate the remainder of bound contamination. This approach may be effective for timely decontamination throughout the emergency phase and continuing into the early recovery phase.

Additional information

The data underlying the figures will also be posted on US EPA's Environmental Dataset Gateway, EPA's official open catalog, at https://edg.epa.gov/metadata/catalog/main/home.page.

CRediT authorship contribution statement

Katherine Hepler: Writing – review & editing, Writing – original draft, Methodology, Investigation, Formal analysis, Data curation, Conceptualization. **Michael D. Kaminski:** Writing – review & editing, Supervision, Resources, Project administration, Methodology, Investigation, Funding acquisition, Formal analysis, Data curation, Conceptualization. **Noemy Escamilla:** Investigation. **Matthew Magnuson:** Writing – review & editing, Methodology, Funding acquisition.

Declaration of competing interest

The authors declare that they have no known competing financial interests or personal relationships that could have appeared to influence the work reported in this paper.

Appendix A. Supplementary data

Supplementary data to this article can be found online at https://doi.org/10.1016/j.heliyon.2024.e34447.

References

[1] IAEA, Chernobyl's legacy: health, environmental and socio-economic impacts and recommendations to the governments of Belarus, the Russian federation and Ukraine, in: The Chernobyl Forum, International Atomic Energy Agency, Vienna, Austria, 2005. INIS-XA–798.
[2] IAEA, The Fukushima Daiichi accident, in: Non-serial Publications, STI/PUB/1710, International Atomic Energy Agency, Vienna, 2015.
[3] J. Nisbet, A.L. Brown, H. Jones, D.J. Rochford, UK recovery handbooks for radiation incidents. HPA-RPD-064, Health Protection Agency, 2009.
[4] K. Brown, K. Mortimer, T. Andersson, A. Duranova, R. Hänninen, G. Ikäheimonen, V. Kirchner, F. Gallay, Generic handbook for assisting in the management of contaminated inhabited areas in Europe following a radiological emergency, EURANOS(CAT1)-TN(06)-09-02, Version 2, Health Protection Agency (2007). Chilton, Oxfordshire, pp. 483.
[5] IAEA, Cleanup of large areas contaminated as a result of a nuclear accident, in: Technical Reports Series No. 300, International Atomic Energy Agency, Vienna, 1989.
[6] I. Stepina Maslova, A. Konoplev, V. Popov, A. Gusarov, F. Pankratov, S. Lee, N. Il'icheva, Fate and transport of radiocesium, radiostrontium and radiocobalt on urban building materials, J. Environ. Radioact. 125 (2013) 74–80.
[7] M. Ochs, D. Mallants, L. Wang, Radionuclide and Metal Sorption on Cement and Concrete, Springer, New York, NY, 2016.
[8] Y.A. Izrael, Radioactive fallout after nuclear explosions and accidents. 245-250, in: Radioactivity in the Environment, vol. 3, Elsevier, 2002.
[9] Utsunomiya S., Furuki G., Ochiai A., Yamasaki S., Nanba K., Grambow B., Ewing R.C., Caesium Fallout in Tokyo on 15th March, 2011 is Dominated by Highly Radioactive, Caesium-Rich Microparticles, 2019. https://doi.org/10.48550/arXiv.1906.00212.
[10] K.H. Larson, J.W. Neel, H.A. Hawthrone, H.M. Mork, R.H. Rowland, L. Baurmash, R.G. Lindberg, J.H. Olafson, B.W. Kowalewsky, Distribution, Characteristics, and Biotic Availability of Fallout, Operation Plumbbob. Projects 37.1, 37.2, 37.2 a, 37.3, and 37.6, 1966 (No. WT-1488). California Univ., Los Angeles. Lab. of Nuclear Medicine and Radiation Biology.
[11] C.F. Miller, The Radiological Assessment and Recovery of Contaminated Areas, Civil Effects Exercise, CEX-57.1, U.S. Naval Radiological Defense Laboratory, San Francisco, CA, 1960.
[12] L.L. Wiltshire, W.L. Owen, Removal of Simulated Fallout from Asphalt Streets by Firehosing Techniques, USNRDL-TR-1049, U.S. Naval Radiological Defense Laboratory, San Francisco, CA, 1965.
[13] L. Warming, Weathering and Decontamination of Radioactivity Deposition Asphalt Surfaces, Riso National Laboratory, 1982. Riso-M-2273.
[14] C. Camarasa-Claret, F. Persin, J. Real, Impact de quelques techniques de lavage sur la decontamination de tuiles et beton contamines par du cesium et du strontium radioactifs, Radioprotection 35 (2001) 13.
[15] J. Real, F. Persin, C. Camarasa-Claret, Mechanisms of desorption of 134Cs and 85Sr aerosols deposited on urban surfaces, J. Environ. Radioact. 62 (2002) 1–15.
[16] M.D. Kaminski, C.J. Mertz, J. Jerden, M. Kalensky, N. Kivenas, M. Magnuson, A case study of cesium sorption onto concrete materials and evaluation of wash agents: implications for wide area recovery, J. Environ. Chem. Eng. 7 (3) (2019) 103140.
[17] L.L. Wiltshire, W.L. Owen, Three Tests of Firehosing Technique and Equipment for the Removal of Fallout from Asphalt Streets and Roofing Materials, U.S. Naval Radiological Defense Laboratory, San Francisco, CA, 1966. USNRDL-TR-1048.

[18] J.D. Owen, Performance Characteristics of Wet Decontamination Procedures, Stoneman II Test of Reclamation Performance, USNRDL-TR-335, vol. 2, U.S. Naval Radiological Defense Laboratory, San Francisco, CA, 1960.

[19] J.L. Dick, T.P. Baker, Monitoring and decontamination techniques for plutonium fallout on large-area surfaces. Operation Plumbbob WT-1512, Air Force Special Weapons Center, Albuquerque, NM, 1961, p. 61.

[20] Jr. Clark, E. D, W.C. Cobbin, Removal of Simulated Fallout from Pavements by Conventional Street Flushers, USNRDL-TR-797, US Naval Radiological Defense Laboratory, San Francisco, CA, 1964.

[21] M.D. Kaminski, S.D. Lee, M. Magnuson, Wide-area decontamination in an urban environment after radiological dispersion: a review and perspectives, J. Hazard. Mater. 305 (2016) 67–86.

[22] D.L. Sparks, Kinetics of ionic reactions in clay minerals and soils, in: N.C. Brady (Ed.), Advances in Agronomy, vol. 38, Academic Press, 1986, pp. 231–266.

[23] R.N. Comans, D.E. Hockley, Kinetics of cesium sorption on illite, Geochem. Cosmochim. Acta 56 (1992) 1157–1164.

[24] J. Roed, Surface deposition of airborne material released by a core-melt accident at a power reactor, in: Riso-M-2274, Risø National Laboratory, 1981.

[25] W.C. Jolin, M.L. Magnuson, M.D. Kaminski, High pressure decontamination of building materials during radiological incident recovery, J. Environ. Radioact. 208 (2019) 105858.

[26] M.D. Kaminski, K. Hepler, M. Magnuson, Pressure Washing Surfaces Contaminated with Fixed and Loose Radioactive Material, U.S. Environmental Protection Agency, Washington, DC, 2023. EPA/600/S-23/042.

[27] K. Hepler, M.D. Kaminski, M. Magnuson, General Filtration Bed Design for Water Contaminated with Radioactive Cesium, U.S. Environmental Protection Agency, Washington, DC, 2023. EPA/600/S-22/043.

[28] W.C. Jolin, C. Oster, M.D. Kaminski, Silicate coating to prevent leaching from radiolabeled surrogate far-field fallout in aqueous environments, Chemosphere 222 (2019) 106–113.

[29] NWS, 2015 Chicago Monthly Precipitation, Temperature and Climate Facts, National Weather Service, 2016. January.

[30] US EPA, Fate of radiological dispersal device (RDD) material on urban surfaces: impact of rain on removal of cesium, in: Tech. Rep, U.S. Environmental Protection Agency, Washington, DC, 2012. EPA/600/R-12/569.

[31] A. Mikelonis, K. Ratliff, S. Youn, Laboratory results and mathematical modeling of spore surface interactions in stormwater runoff, J. Contam. Hydrol. 235 (2020) 103707.

[32] R.M. Cornell, Adsorption of cesium on minerals: a review, Journal of Radioanalytical and Nuclear Chemistry. Articles 171 (1993) 483–500.

[33] R.A. Bowling, A theoretical review of particle adhesion, in: K.L. Mittal (Ed.), Particles on Surfaces 1, Springer, Boston, MA, 1988.

[34] M. Kaminski, C. Mertz, L. Ortega, N. Kivenas, Sorption of radionuclides to building materials and its removal using simple wash solutions, J. Environ. Chem. Eng. 4 (2016) 1514–1522.

[35] W.C. Jolin, M.L. Magnuson, M.D. Kaminski, High pressure decontamination of building materials during radiological incident recovery, J. Environ. Radioact. 208 (2019) 105858.

[36] J. Bardina, Methods for surface particle removal: a comparative study, in: K.L. Mittal (Ed.), Particles on Surfaces 1, Springer, Boston, MA, 1988.

[37] M. Elimelech, C.R. O'Melia, Kinetics of deposition of colloidal particles in porous media, Environ. Sci. Technol. 24 (10) (1990) 1528–1536.

[38] R. Musselman, T. Yarbrough, Shear stress[TM] cleaning for surface departiculation, J. Environ. Sci. 30 (1) (1987) 51–56.

[39] S. Rajupet, A.A. Riet, Q. Chen, M. Sow, D.J. Lacks, Relative importance of electrostatic and van der Waals forces in particle adhesion to rough conducting surfaces, Phys. Rev. 103 (4) (2021) 042906.

[40] W.C. Jolin, C. Oster, K. Hepler, M. Magnuson, M.D. Kaminski, Effects of aging and decontamination pressure on the penetration of radionuclides into concrete – 18418, in: Proceedings of 2018 WM Symposia, (Phoenix, AZ), Waste Management Symposia, 2018.

[41] K. Andersson, B. Torstenfelt, B. Allard, Sorption and diffusion studies of Cs and I in concrete. Tech. Rep. SKBF/KBS 83-13, Kaernbraenslesaekerhet, Stockholm, 1983, p. 20.

[42] A. Atkinson, A.K. Nickerson, Diffusion and sorption of cesium, strontium, and iodine in water-saturated cement, Nucl. Technol. 81 (1988) 100–113.

[43] E.B. Farfan, S.P. Gaschak, A.M. Maksymenko, E.H. Donnelly, M.D. Bondarkov, G.T. Jannik, J.C. Marra, Assessment of 90Sr and 137Cs penetration into reinforced concrete (extent of "deepening") under natural atmospheric conditions, Health Phys. 101 (2011) 311–320.

[44] T. Kono, F.W. Barham, A water fountain for decontamination of used vials and test tubes, Anal. Biochem. 63 (2) (1975) 592–594, https://doi.org/10.1016/0003-2697(75)90385-1.

[45] S. Lee, K. Hall, S. Hudson, P. Lemieux, M. Magnuson, J. Mitchell, E. Snyder, T. Stilman, M. Hannant, R. James, A. Gregg, M. Langton, Z. Willenberg, A. Dindal, Evaluation of Low-Tech Outdoor Decontamination Methods Following Wide Area Radiological/Nuclear Incidents, U.S. Environmental Protection Agency, Washington, DC, 2017. EPA/600/R-17/021.

[46] M. Kaminski, N. Kivenas, C. Oster, W. Jolin, M. Magnuson, K. Hepler, Integrated wash-aid, treatment, and emergency reuse system (IWATERS) for strontium contaminations-17390, in: In Proceedings of the 2017 WM Symposia, (Phoenix, AZ), Waste Management Symposia, 2017.

[47] W.C. Jolin, M.D. Kaminski, Developing Surrogate Far-Field Nuclear Fallout and its Rapid Decontamination from Aircraft Surfaces (No. ANL/SSS-19/1), Argonne National Lab.(ANL), Argonne, IL (United States), 2019.

[48] S. Lee, T. Boe, K. Hall, S. Hudson, M. Ierardi, P. Lemieux, M. Magnuson, A. Mikelonis, J. Mitchell, T. Stilman, J. Archer, M. Hannant, R. James, Z. Willenberg, K. McConkey, Evaluation of Low-Tech Outdoor Decontamination Methods Following Wide Area Radiological/Nuclear Incidents, U.S. Environmental Protection Agency, Washington, DC, 2019. EPA/600/R-19/001.